Toxicology in Vitro 60 (2019) 1–11

Contents lists available at ScienceDirect

Toxicology in Vitro

journal homepage: www.elsevier.com/locate/toxinvit

Development and validation of bioengineered intestinal tubules for translational research aimed at safety and efficacy testing of drugs and nutrients

Paulus G.M. Jochems[a], Jeroen van Bergenhenegouwen[a,b], Anne Metje van Genderen[a], Sophie T. Eis[a], Livia J.F. Wilod Versprille[a], Harry J. Wichers[c], Prescilla V. Jeurink[a,b], Johan Garssen[a,b], Rosalinde Masereeuw[a,*]

[a] Division of Pharmacology, Utrecht Institute of Pharmaceutical Sciences, Utrecht University, Universiteitsweg 99, Utrecht 3584 CG, the Netherlands
[b] Nutricia Research, Danone Nutricia Research, Global Center of Excellence Immunology, Utrecht 3584 CT, the Netherlands
[c] Wageningen Food & Biobased Research, Wagening University, Wageningen 6708 PB, the Netherlands

ARTICLE INFO

Keywords:
Caco-2
Small intestine
In vitro
Microfluidic and screening

ABSTRACT

Currently used intestinal cell models have limited translational value, therefore, development of novel *in vitro* intestinal models that recapitulate the human *in vivo* setting more closely are of interest. Here, an advanced intestinal model was developed by the incorporation of physiological parameters, such as extracellular matrix (ECM) elements and shear stress, to cultured Caco-2 cells in a 3-dimensional environment. Caco-2 cells grown on ECM-coated hollow fiber membranes (HFM) under physiological shear stress show an improved phenotype, as demonstrated by the presence of enterocytes, goblet, Paneth, enteroendocrine and stem cells. Additionally, this model showed signs of an improved morphology due to the appearance of villi-like structures. Similar to epithelial cells grown on Transwells™, the current model remains easy to use, cost efficient and allows apical and basolateral access. The bioengineered intestinal tubule was validated by exposure to *Clostridium difficile* toxin A, the leading cause of healthcare-associated diarrhea. The loss of the tight junction network was supported by an increase in inulin-FITC leakage and the number of goblet cells increased, in agreement with clinical findings. In addition to toxicity screening, the bioengineered intestinal tubules are considered useful for drug and nutrient safety and efficacy testing.

1. Introduction

To bring novel drugs, nutraceuticals or food ingredients to the market, regulations require toxicity and efficacy data. Before moving into animal models, new compounds are regularly screened using *in vitro* models to determine their toxic effects on cell growth and function, and, if relevant, for efficacy such as a positive effect on gut integrity. However, *in vitro* models are only simplistic representations of complex physiological systems, with limited translational value (Honek, 2017). More physiological relevant *in vitro* models have various advantages, such as small amounts of chemicals that are needed for testing and a reduction in animal experimentation (Jain et al., 2017). The latter finds international support, as replacement, reduction and refinement (the three R's) of animal experiments wherever possible is anchored in European legislation (Holley et al., 2016). Driven by the need to enhance clinical predictivity, more complex models are currently being developed. However, as complexity and physiological relevance increase, reproducibility and throughput decrease (Funk and Roth, 2017). Finding the perfect balance between these parameters is challenging. As the oral route is the most frequently used route for nutrition and drugs administration, *in vitro* models for the small intestine are of interest as well (Bardal et al., 2010).

Gastrointestinal toxicity is a commonly observed side effect of medical treatment and often associated with chemotherapy, non-steroidal anti-inflammatory, cardiovascular or psychotropic medication, which results in constipation or disruption of the intestinal epithelial barrier (Pusztaszeri et al., 2007; Boussios et al., 2012; Philpott et al., 2014). Of importance, a compromised intestinal barrier or “leaky

Abbreviations: Hollow fiber membranes, (HFM); Transwell™, (TW); Toxin A, (Tox A); Zonula occludens-1, (ZO-1); Mucin-2, (MUC2); Chromogranin A, (ChrA); Lysozyme, (Lys); Polyether sulfone, (PES); Extracellular matrix, (ECM); L-3,4-di-hydroxy-phenylalanine, (L-Dopa); Alkaline phosphatase, (ALP).

* Corresponding author.
E-mail address: r.masereeuw@uu.nl (R. Masereeuw).

https://doi.org/10.1016/j.tiv.2019.04.019
Received 30 November 2018; Received in revised form 2 April 2019; Accepted 17 April 2019
Available online 06 May 2019

gut" is associated with various diseases and disorders in both humans and animals (Stewart et al., 2017). The most commonly used *in vitro* tool to study the small intestinal barrier is the cultivation of Caco-2 cells on Transwell™ (TW) inserts (Press and Di Grandi, 2008). Caco-2 cells are praised for their spontaneous differentiation into a small intestinal phenotype and capacity to mimic *in vivo* intestinal permeability when grown to full confluency (Press and Di Grandi, 2008; Meunier et al., 1995; Sun et al., 2008). However, the conventional Caco-2 model also has some limitations, such as their colon carcinoma origin, differentiation into solely absorptive enterocytes, sensitivity to variations in culture conditions, leading to inter-laboratory differences (Hilgendorf et al., 2000; Lea, 2015). Recently, the use of (stem cell or biopsy-derived) organoids are considered an attractive alternative. Organoids have the advantage that they can differentiate into all small intestinal cell types and self-organize into well-defined structures (Le Ferrec et al., 2001; Zachos et al., 2016). However, organoids are still in the developmental stage and several hurdles remain to be solved. For instance, organoids cultured in a 3-dimensional fashion grow inside-out with the apical barrier and lumen on the inside and therefore difficult to access, which makes them unusable for transport studies (Zachos et al., 2016; Chen et al., 2018).

Simultaneously, the field of (microfluidic) organ on a chip technology has received great interest. These novel technologies offer an intermediate between original TW cultures and organoids by having increased complexity. They have shown to improve cell differentiation and polarization, resulting in closer mimicking of the physiology of the relevant organ and therefore promising to accelerate translation to the *in vivo* situation (Huh et al., 2012). Increasing complexity in novel small intestinal models was recently attained by culturing cells under physiological relevant flow and/or by the addition of an extracellular matrix (ECM) (Kim et al., 2012; Trietsch et al., 2017; Kim and Ingber, 2013). Physiological intestinal fluid flow varies between 0.002 and 0.08 dyne/cm^2, depending on *e.g.* digesta properties (Lentle and Janssen, 2008). Application of flow on Caco-2 cultures can result in villi-formation and differentiation into the four main intestinal epithelial cell types, enterocytes, goblet cells, enteroendocrine cells and Paneth cells (Kim and Ingber, 2013). Incorporation of elements of the ECM, important in cell signaling and differentiation, further enhanced Caco-2 cell differentiation as observed *via* an increased activation of brush border enzyme activity (Li and Thompson, 2003; Yue, 2014; Basson et al., 1996a).

Most novel and more complex models make use of flat membranes, lacking the support to form intestinal tube-like structures. However, it has been shown in the field of tissue engineering, that proliferation and differentiation of biological tissues are partly regulated by local geometrical properties (Clause et al., 2010). Hollow fiber membranes (HFM), *e.g.* from the stable and low-cost biocompatible material polyether sulfone (PES), have shown to be a promising *in vitro* platform for tube-like tissue development representing multiple organs (Chen et al., 2018; Azadbakht et al., 2011; Schophuizen et al., 2015). HFM support cells to grow in a 3-dimensional tubule, more closely mimicking the biological structure of the intestine and potentially accelerating differentiation of Caco-2 cells as compared to cells grown on TW inserts (Deng et al., 2013).

Altogether, combining physiological parameters and HFM constructs in one model seems promising for novel drugs, nutraceuticals, food ingredients and toxin screening. Here, we hypothesize that the combination of these parameters will advance Caco-2 polarization and differentiation, and leads to a model more closely mimicking intestinal physiology. Such models can be applied to evaluate the effects of potent intestinal barrier disrupters, such as the *Clostridium difficile* secreted toxin A.

2. Material and methods

2.1. Chemicals

All chemicals were purchased from Sigma-Aldrich (Zwijndrecht, The Netherlands) unless stated otherwise.

2.2. Cell culture

Caco-2 cells (ATCC, Wesel, Germany) were maintained in high glucose Dulbecco's Modified Eagle Medium (Gibco) with fetal calf serum (10% *v*/v) and penicillin and streptomycin (1% v/v) supplementation. Media was refreshed every 2–3 days, and cells were passaged and seeded on HFM when reaching 80–90% confluency.

2.3. Hollow fiber membrane extracellular matrix and seeding

Two types of HFM were evaluated: the MicroPES type TF10 hollow fiber capillary membranes (Membrana GmbH, Wuppertal, Germany) and SENUOfil type H-MF-0,2 hollow fiber capillary membranes (SENUOFIL, Tianjin, China). 1.5 mL Eppendorf tubes were used to perform HFM ECM coating and Caco-2 seeding. HFM were cut in 4.5 cm pieces and sterilized in 70% (*v*/v) EtOH for 30 min. Next, HFM were washed in PBS and put in filter-sterilized L-3,4-di-hydroxy-phenylalanine (L-Dopa, 2 mg.mL^{-1} in 10 mM Tris buffer, pH 8.5). Tubes containing HFM were incubated at 37 °C and turned 90° every hour for five consecutive hours to allow full polymerization of L-Dopa. After drying at 37 °C for 5 min, HFM were washed with PBS and put in human collagen IV solution (25 μg.mL^{-1} in PBS) for another incubation at 37 °C for 2 h turning. HFM 90° every 30 min. HFM were dried for 5 min at 37 °C and unbound human collagen IV was washed off with PBS. Finally, HFM were washed and stored in PBS awaiting cell seeding for a maximum of 4 days.

Caco-2 cells were washed, trypsinized and resuspended in culture medium (Dulbecco's Modified Eagle Medium (Gibco) supplemented with fetal calf serum (10% v/v) and penicillin and streptomycin (1% v/v)) at desired concentrations varying from 0.5–1.5*10^6 cells/HFM referred to as cell suspension. For initial cell seeding, HFM were added to 1.5 mL cell suspension in Eppendorf tubes and incubated at 37 °C for four h, turned 90° every h. Thereafter, seeded ECM-HFM were added to a six well plate and 4 mL of culture medium was added. Cells were allowed to grow to confluency for a period of 21 days in a 37 °C incubator. Shear stress was applied through incubation of the six-well plates on a 2-dimensional rocking platform (VWR, Breda, The Netherlands) with a speed rate of 1 rotation per minute at an angle of 10^o for different durations varying between 0 and 21 days of the entire culture time. During shear stress conditions the medium was increased to 6 mL to ensure medium coverage during rocking. Medium was refreshed every 2–3 days.

2.4. Transwell™ extracellular matrix and seeding

TW were coated with ECM. First, TW were washed with PBS followed by sterilization for 30 min in 70% (*v*/v) EtOH. After washing in PBS, filter-sterilized L-3,4-di-hydroxy-phenylalanine (L-Dopa, 2 mg.mL^{-1} in 10 mM Tris buffer, pH 8.5) was added on the apical and basolateral membrane. TW were incubated at 37 °C for five consecutive hours to allow full polymerization of L-Dopa. After drying at 37 °C for 5 min, TW were washed with PBS and incubated with human collagen IV solution (25 μg.mL^{-1} in PBS) added to both the apical and basolateral side of the membrane for another incubation at 37 °C for 2 h. TW were dried for 5 min at 37 °C and unbound human collagen IV was washed off with PBS. TW were kept in PBS awaiting seeding.

TW were seeded at a density of 0.56*10^6 cells/well and maintained in culture for 21 days in 37 °C. During the final 7 days, plates with the TW were put on a 2-dimensional rocking platform with a speed rate of 1 rotation per minute at an angle of 10^o. *medium* was refreshed every

2–3 days.

2.5. Immunofluorescent staining

To investigate epithelial-layer integrity, phenotypical and morphological characteristics, immunostainings were performed. Cells were fixed using Carnoy's solution (60% EtOH, 30% Chloroform, 10% glacial acetic acid (*v/v*)) and permeabilized (0.3% (v/v) Trition X-100 in HBSS). To prevent non-specific binding of antibodies, cells were incubated with block solution (2% (*w/v*) bovine serium albumin (BSA) fraction V and 0.1% (v/v) Tween-20 in HBSS). Fixed cells were incubated with primary antibodies, diluted in block solution, used were tight junction protein, zonula occludens-1 (ZO-1, 1:1000) (Thermo Fisher Scientific, Bleiswijk, The Netherlands), goblet cell marker, Mucin-2 (MUC2, 1:200) (Abcam, Cambridge, United Kingdom), enteroendocrine cell marker, chromogranine A (ChrA, 1:100) (Abcam), Paneth cell marker, lysosyme (Lys, 1:200) (Abcam) and stem cell marker, leucine-rich repeat-containing G-protein coupled receptor 5 ($LGR5^+$, 1:400) (Abcam) for 2 h. This was followed by incubation with goat-anti-mouse 488 (1:200; Thermo Fisher Scientific) or goat-anti-rabbit 594 (1:200; Abcam) as secondary antibodies. Finally, HFM were mounted using Prolong gold containing DAPI (Cell signaling technology, Leiden, The Netherlands) for nuclei staining. Images were acquired using the Leica TCS SP8 X (Leica Biosystems, Amsterdam, The Netherlands).

2.6. Inulin-FITC leakage assay

To quantify paracellular permeability, an inulin-FITC (0.1 $mg.ml^{-1}$ in PBS) leakage assay was performed. The HFM was connected in a custom-made 3D printed cytocompatibility polyester chamber after prewashing the chamber with PBS. HFM was connected to glass cannula (inner diameter 120–150 μm) DMT Trading, Aarhus, Denmark) using microsuture silk (Pearsalls Limited, Taunton, UK). To confirm leak tight attachment, the HFM was perfused with PBS. The apical compartment of the module was filled with 300 μL PBS. Thereafter, the HFM was perfused with inulin-FITC at a speed rate of 0.1 mL/min for 10 min using Terumo Syringe Pump TE-311 (Terumo, Leuven, Belgium). Samples were taken from the apical compartment. For the TW, 0.5 mL of inulin-FITC solution was put in the apical compartment and 1.5 mL PBS was added to the basolateral compartment. After 10 min, samples were taken from the basolateral compartment. Fluorescence of the samples was measured at excitation wavelength of 492 nm and emission wavelength of 518 nm using Tecan infinite M200PRO plate reader (Tecan Austria GmbH). As HFM and TW properties can deviate slightly, results are shown relative to ECM-coated unseeded construct as negative control to correct for day to day experimental variation.

2.7. Alkaline phosphatase activity and protein content

Alkaline phosphatase (ALP) activity was measured as enterocyte differentiation marker, using Amplite™ Fluorimetric Alkaline Phosphatase assay kit (AAT Bioquest, Sunnyvale, USA). The assay was performed according manufacturer protocol with minor adaptations. HFM were incubated for 15 min at 37 °C; thereafter, absorbance was measured at 400 nm with iMARK™ microplate absorbance reader (Bio-rad, Veenendaal, The Netherlands). ALP activity was normalized for protein content using Pierce BCA protein assay kit (Thermo Fisher Scientific). Assay was performed according manufacturer protocol with minor adaptations. HFM were incubated for 30 min at 37 °C. Thereafter, absorbance was measured at 600 nm with iMARK™ microplate absorbance reader (Bio-rad).

2.8. Clostridium difficile toxin A exposure

After 21 days of cultivation, bioengineered intestinal tubes were exposed to toxin A (Tox A) (Quadratech Diagnostics Ltd., Epsom, United Kingdom) for 24 h. Tox A was dissolved and stored according manufacturer at 4 °C. Tox A was dissolved in medium and HFM were exposed at different concentrations 0.5, 0.25, 0.125 μg/mL.

2.9. Statistical analysis

Every experiment was at least performed in triplicate, results are depicted as mean ± standard error of the mean. Statistical analysis was performed in Graphpad version 5 using one-way ANOVA followed by a Tukey's post-hoc test. A *P*-value of < 0.05 was considered significantly different.

3. Results

3.1. Hollow fiber membranes support 3-dimensional Caco-2 cultures

To determine the effect of the microenvironment on cell monolayers, the barrier formation was evaluated by immunofluorescent staining of the tight junction protein ZO-1 and inulin-FITC leakage over the epithelial barrier. The cell differentiation was analyzed by immunofluorescent staining of MUC2, as marker for the goblet cell phenotype. Firstly, two different sizes of HFM were tested, both composed of PES. The smaller microPES fiber had an inner diameter of 300 μm, wall thickness of 200 μm, pore size of 0.5 μm and curvature of 0.0029 κ whereas the bigger SENUOfil had an inner diameter of 400 μm, thickness of 200 μm, pore size of 0.2 μm and curvature of 0.0025 κ (Fig. 1A).

Caco-2 cells cultured on the microPES and SENUOfil HFM developed a differentiated and polarized monolayer as shown by positive ZO-1 staining (Fig. 1B). ZO-1 is expressed in the lateral membranes in close proximity of the apical surface of epithelial cells, suggesting polarization. This localization was confirmed in a cross-section of the HFM, also demonstrating that Caco-2 cells attached with their basolateral surface to the HFM (see supplementary data for image). The cells form tightest barriers on SENUOfil HFM as confirmed by inulin-FITC leakage which was significantly lower compared to unseeded control (11.8 fold) (Fig. 1C). Caco-2 cells on both constructs stained positive for MUC2 (Fig. 1B), indicating the presence of the goblet cell phenotype in the Caco-2 population.

Next, the relevance of applying an ECM were evaluated. Here, we used a double coating strategy by adding first a layer of L-3,4-di-hydroxy-phenylalanine (L-Dopa) on the HFM followed by a layer of human collagen IV (Fig. 3A) first developed by Ni et al. and later optimized by Schophuizen et al. (Schophuizen et al., 2015; Ni et al., 2011).

Nuclei staining (Fig. 2B) revealed that Caco-2 cells do not depend on the ECM coating for adherence, as both the ECM-coated as well as the ECM-uncoated HFM were completely covered with cells. ZO-1 (Fig. 2B), however, was more prominently formed in the ECM-coated HFM. This observation was supported by the inulin-FITC leakage data (Fig. 2C, right). Both HFM showed a significantly lower leakage compared to its unseeded control was measured. ECM-coating by itself did not affect the inulin-FITC leakage of the HFM (Fig. 2C, left). Furthermore, MUC2 staining was less abundant (Fig. 2B) in the absence of the ECM-coating indicating the importance of the ECM in cell differentiation.

Caco-2 cells can spontaneously differentiate into a small-intestinal phenotype upon reaching confluency (Lea, 2015), which requires a differentiation process of 2–3 weeks (Ferruzza et al., 2012). Here, we evaluated different seeding densities for optimal small-intestinal phenotype monolayer formation.

In contrast to the TW system, where gravity assures cells to settle on the insert, it is important to take into account that not all Caco-2 cells in the seeding suspension will attach to the HFM (attachment of 82.2% ± 12.1%). When a seeding density of $1.0*10^6$ cells/HFM was used, the ZO-1 network was most apparent in comparison with $0.5*10^6$ and $1.5*10^6$ cells/HFM, whereas no clear difference was observed for

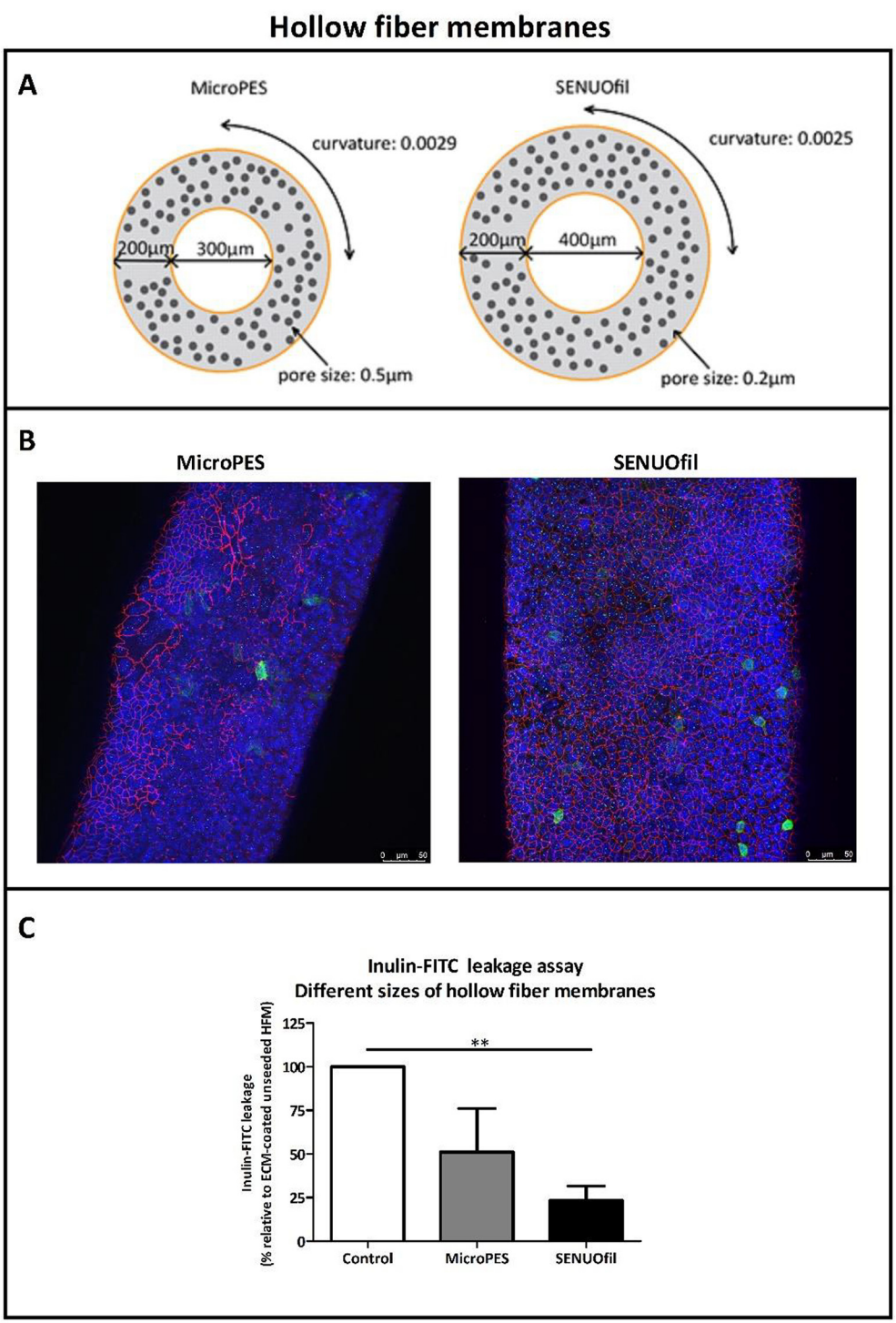

Fig. 1. Caco-2 cells form tightest monolayers on SENUOfil HFM. (A) illustrative image of the two different HFM, (B) confocal microscopic image of extracellular matrix coated Caco-2 seeded on microPES (left) and SENUOfil (right) hollow fiber membranes. DAPI was used to stain the nuclei (blue), mucin-2 (MUC2) to stain goblet cells (green) and zonula occludens-1 (ZO-1) to stain for tight junction formation (red). Images are shown as maximal intensity projection. (C) Inulin-FITC paracellular leakage data are presented relative to control (extracellular matrix coated unseeded HFM) as mean ± SEM of at least 3 independent experiments.** $P < 0.005$ using one-way ANOVA. (For interpretation of the references to colour in this figure legend, the reader is referred to the web version of this article.)

the presence of MUC2-positive cells (Fig. 3A). Cell seeding densities of $0.5*10^6$ and $1.0*10^6$ cells/HFM resulted in an improved barrier formation (Fig. 3B) compared to unseeded HFM control, with the latter density showing the strongest effect. Therefore, an optimal seeding density of $1.0*10^6$ cells/HFM was selected.

The final parameter in the microenvironment to assess was the inclusion of physiologically relevant shear stress. The human small intestine is continuously exposed to shear stress, ranging from 0.08–0.002 dyne/cm^2 (Kim et al., 2012). We evaluated shear stress (0.006 dyne/cm^2) durations varying from 0 to 21 days during the entire culture time.

Shear stress led to further differentiation, including the appearance of villi-like structures (Fig. 4B, video in supplementary data[1]). All different shear stress durations allowed for the differentiation of cells, as supported by MUC2 staining (Fig. 4B). Seven day exposures to shear stress led visually to the most abundant villi-like structures (Suppl. Video 1[1]). Quantification of permeability (Fig. 4C) showed that shear stress had no effect on the barrier formation as all different durations led to a significant decrease in FITC-inulin leakage compared to

[1] Supplementary video shows a bioengineered intestinal tubule (ECM-coated Caco-2 seeded HFM with shear stress exposure of 0.006 dyne/cm^2 from day 14–21). Tight junction network is shown in red presenting zonula occludens-1 staining, goblet cells are shown in green by mucin-2 staining and nuclei are shown in blue by DAPI staining.

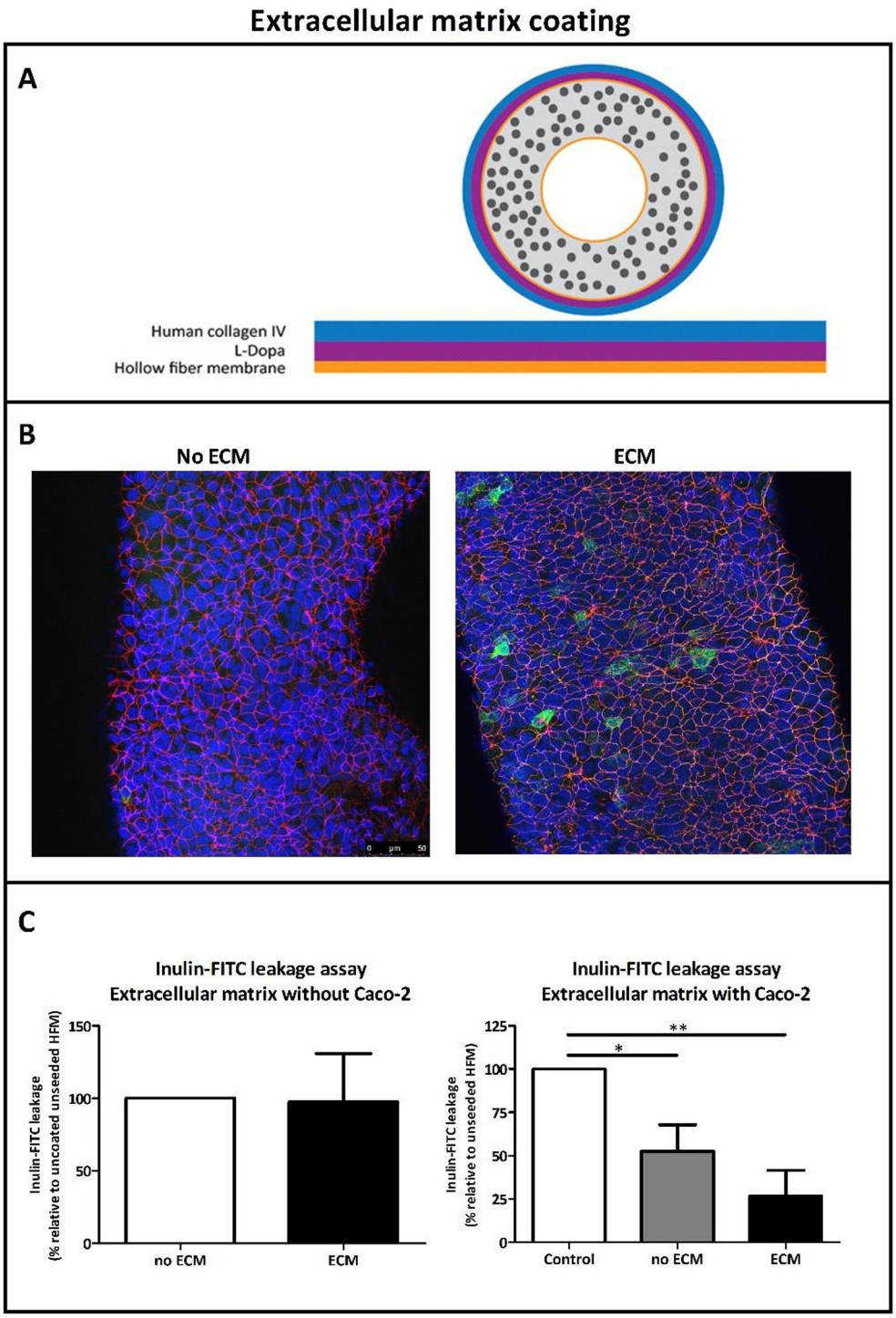

Fig. 2. Caco-2 cells on extracellular matrix (ECM) coated hollow fiber membranes (HFM) form tighter monolayers and higher number of goblet cells differentiation. (A) illustrative image of the L-3,4-di-hydroxy-phenylalanine (L-Dopa) and human collagen IV ECM coating on the HFM, (B) confocal microscopic image of ECM uncoated (left) and coated (right) Caco-2 seeded hollow fiber membrane. DAPI was used to stain the nuclei (bleu), mucin-2 (MUC2) to stain goblet cells (green) and zonula occludens-1 (ZO-1) to stain for tight junction formation (red). Images are shown as maximal intensity projection. (C) Inulin-FITC paracellular leakage, comparison of ECM uncoated and coated unseeded HFM (left) and a comparison of ECM uncoated and coated seeded HFM (right). Data are presented relative to unseeded control HFM as mean ± SEM of at least 3 independent experiments and was tested for significance using one-way ANOVA, $*P < 0.05$, $** P < 0.005$. (For interpretation of the references to colour in this figure legend, the reader is referred to the web version of this article.)

unseeded control HFM. Based on these findings, we decided to proceed with a shear stress duration of 7 days after 14 days of static cultures.

The overall decision tree of our model development leading to bioengineered intestinal tubules is presented in Fig. 5.

As mentioned before, the capacity to form a functional barrier allowing selective transport from the apical to basolateral side is an important aspect of the bioengineered intestinal tubules. To compare the experimental setup *versus* the established TW model, an inulin-FITC leakage assay was performed in both models. Both the TW and bioengineered intestinal tubules demonstrated a good epithelial cell barrier function and no differences were observed when leakage was compared between TW and the bioengineered intestinal tubules (suppl. Fig. 2).

After the microenvironment of the bioengineered intestinal tubules had been defined, cell differentiation was evaluated more elaborately. The model was tested for the presences of enterocytes-like cells with ALP activity assay. Presence of enteroendocrine cells, Paneth cells and stem cells were shown by immunostaining for ChrA, Lys and LGR5$^+$, subsequently (Fig. 6).

Caco-2 cells cultivated in the model, showed a ALP activity of 0.1577 mU/μg protein indicating an enterocyte-like differentiation. Positive staining for ChrA, Lys and LGR5$^+$ comfirmed differentiation of enteroendocrine, Paneth and stem cells subsequently, comfirming the presence of all four main cell types of the small intestine present in the model, and surprisingly even stem cells.

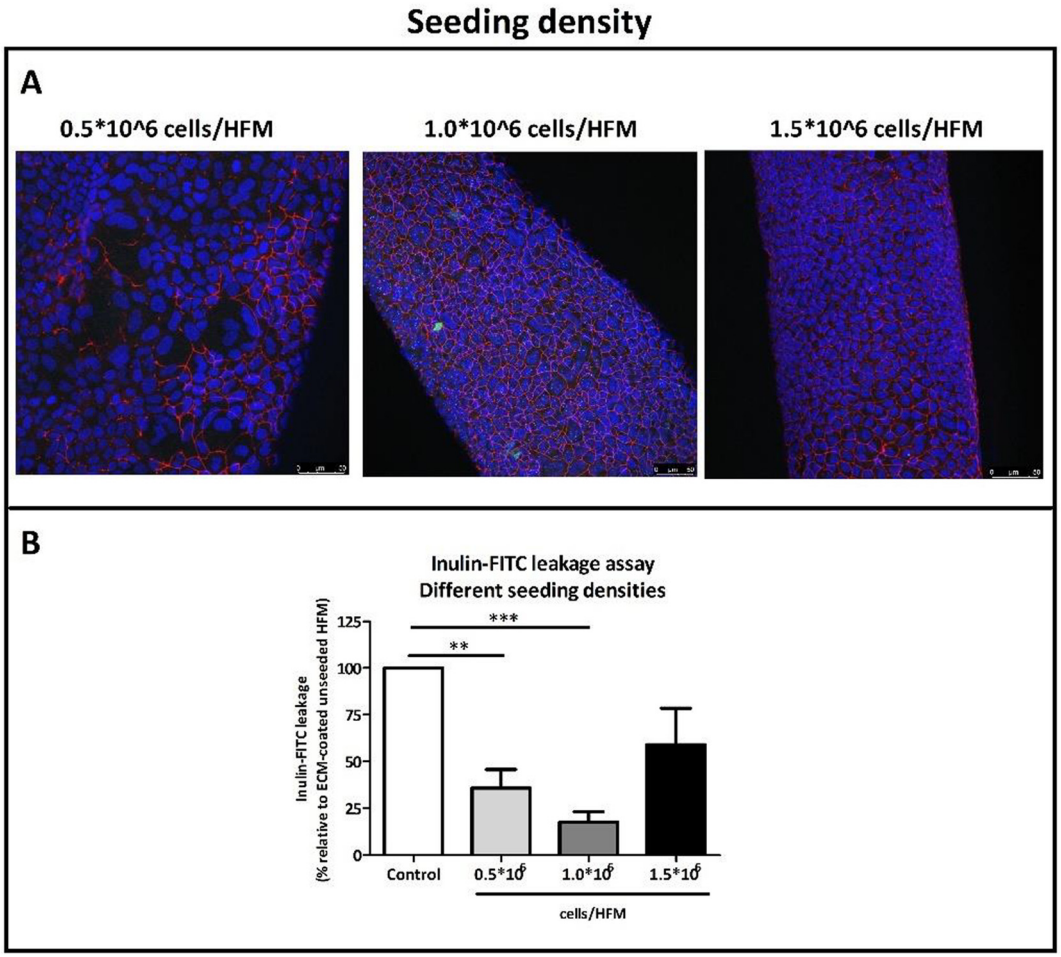

Fig. 3. Caco-2 cells seeded in a concentration of $1.0*10^6$ cells/hollow fiber membranes (HFM) form tight monolayers with apparent zonula occludens-1 (ZO-1) network. (A) confocal microscopic image of 21 days cultivated ECM-coated HFM with different seeding density, $0.5*10^6$ cells/HFM (left), $1.0*10^6$ cells/HFM (middle) and $1.5*10^6$ cells/HFM (right). DAPI was used to stain the nuclei (bleu), mucin-2 (MUC2) to stain goblet cells (green) and ZO-1 to stain for tight junction formation (red). Images are shown as maximal intensity projection. (B) Inulin-FITC paracellular leakage, data are presented relative to control (ECM-coated unseeded HFM) as mean ± SEM of at least 3 independent experiments. $^{**}P < 0.005$, $^{***}P < 0.001$ using one-way ANOVA. (For interpretation of the references to colour in this figure legend, the reader is referred to the web version of this article.)

3.2. The bioengineered intestinal tubule is a suitable model for toxin screening

After having the bioeingineered intestinal tubulus model established, its applicability was tested for its suitability in barrier disruption experiments using toxin exposure. For this, toxin A (Tox A), a toxin produced by the gram-positive bacteria *Clostridium difficile* was used. *Clostridium difficile* infections cause 15–25% of the antibiotic-associated diarrhea through potent barrier disruption (DePestel and Aronoff, 2013).

After Tox A exposure, the ZO-1 network of the intestinal tubules was completely disrupted for all concentrations tested (Fig. 7A). Inulin-FITC leakage showed a significant barrier formed for medium and all Tox A exposed HFM compared to the unseeded control HFM. The highest concentration 0.5 µg/mL Tox A showed a significant increase in inulin-FITC leakage compared to medium and the lowest Tox A concentration, showing the potency of Tox A to compromise the intestinal barrier.

The presence of a cell layer in the HFM already posed a significant barrier to leakage of inulin-FITC. Exposure to Tox A seemed to show a trend towards increased leakage, although this did not reach significance (Fig. 7B). Furthermore, the Caco-2 population remained positive for MUC2 staining. The number of goblet cells even seemed slightly increased compared to unexposed Caco-2 cells (Fig. 7A), suggesting more mucus production. In conclusion, Tox A disrupts the tight junction network, increased inulin-FITC leakage and seemed to slightly upregulate MUC2 positive cells.

4. Discussion

In comparison to the conventional 2-dimensional TW inserts, the HFM constructs supported the cells to grow in more physiological 3-dimensional tube-like structures. Cells grown on these constructs differentiated and polarized with distinct basolateral and apical membranes. Moreover, the HFM tubuli are accessible from the apical and basolateral side necessary to study trans-epithelial transport. We compared two sizes of HFM with slight differences in pore size and curvature. It is known from the field of tissue engineering that proliferation and differentiation of biological tissues are partly regulated by local geometrical features, such as curvature and pore size (Alias and Buenzli, 2017; Murphy, 2010). Pore size is essential for sufficient nutrient diffusion, waste removal and cell adhesion (Murphy and Haugh, 2010). Insufficient nutrient diffusion and waste removal can result in *e.g.* inhibition of proliferation (McKee and Chaudhry, 2017). In turn, curvature can influence cytoskeletal forces acting on the nucleus. Altering nuclear shapes affects cellular function and can therefore alter polarization and differentiation (Werner et al., 2017; Webster et al., 2009). The results demonstrated that SENUOfil HFM is the preferred material, as these showed a significantly improved epithelial barrier

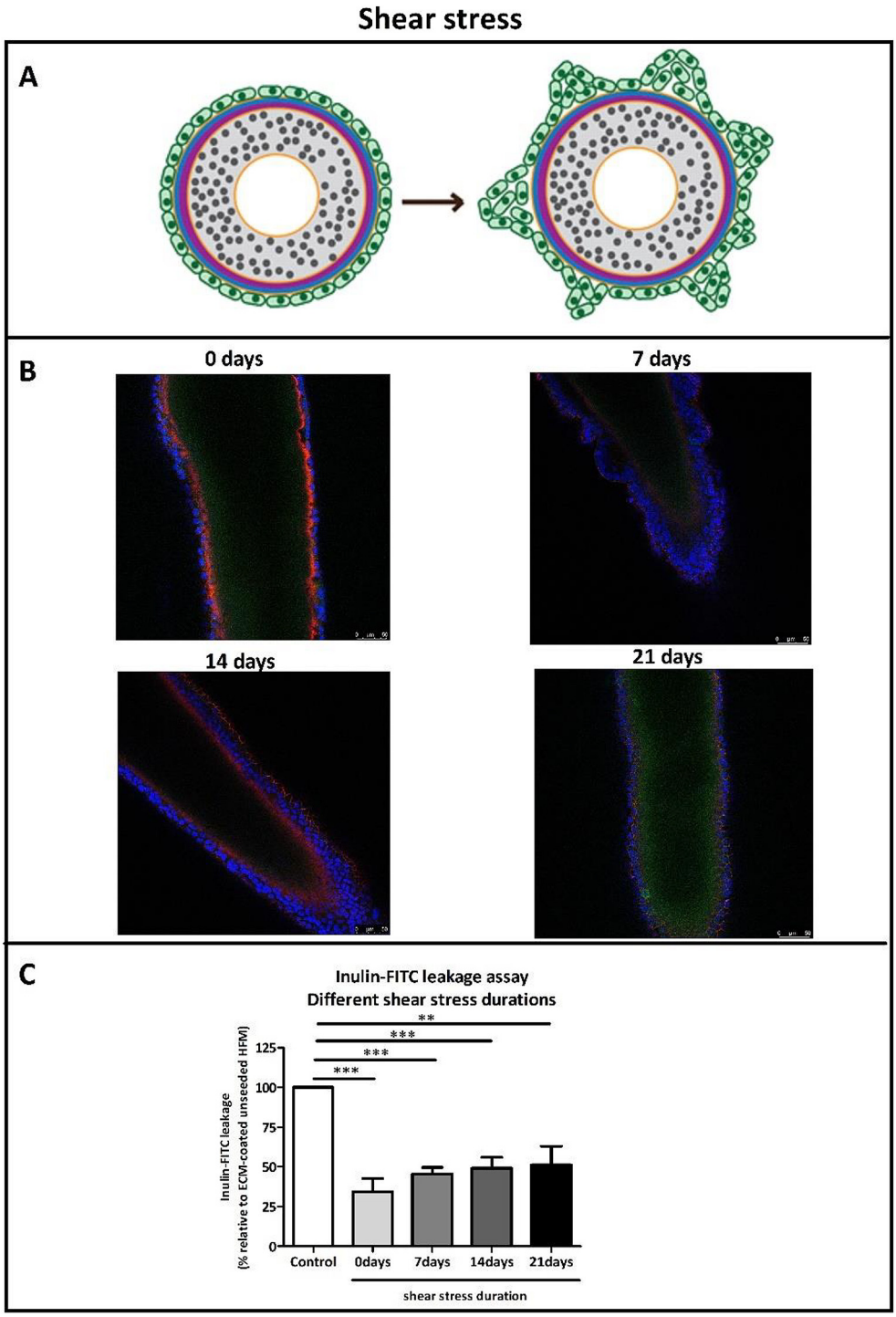

Fig. 4. Caco-2 cells seeded on extracellular matrix coated hollow fiber membranes exposed to a shear stress of 0.006 dyne/cm^2 for the final 7 days result in tubules with most apparent villi-like structures. (A) representative confocal microscopic image of coated Caco-2 seeded hollow fiber membrane with 7 days of shear stress, (B) representative confocal microscopic image of coated Caco-2 seeded hollow fiber membrane with 0–21 days of shear stress and In blue the DAPI staining of nuclei, immunostaining in green for mucin-2 and in red for zonula occludens-1. (C) Inulin-FITC paracellular leakage, data are presented relative to control as mean ± SEM of at least 3 independent experiments and was tested for significance to unseeded control HFM. $^{**}P < 0.005$, $^{***}P < 0.001$ using one-way ANOVA. (For interpretation of the references to colour in this figure legend, the reader is referred to the web version of this article.)

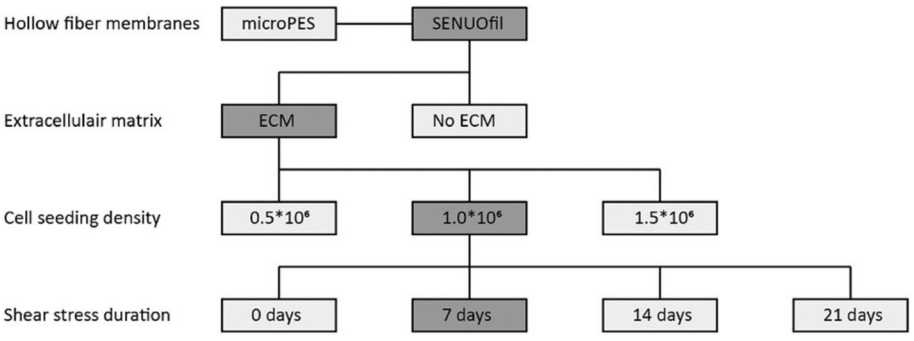

Fig. 5. Decision tree of considerations for the microenvironment of the bioengineered intestinal tubules. The final settings for the bioengineered intestinal tubules consist of the SENUOfil HFM with double coating of L-DOPA and human collagen IV. Cell seeding density was set to be 1.0*10^6 cells/HFM and the cells are exposed to a shear stress of 0.006 dyne/cm^2 during the final 7 days of culture.

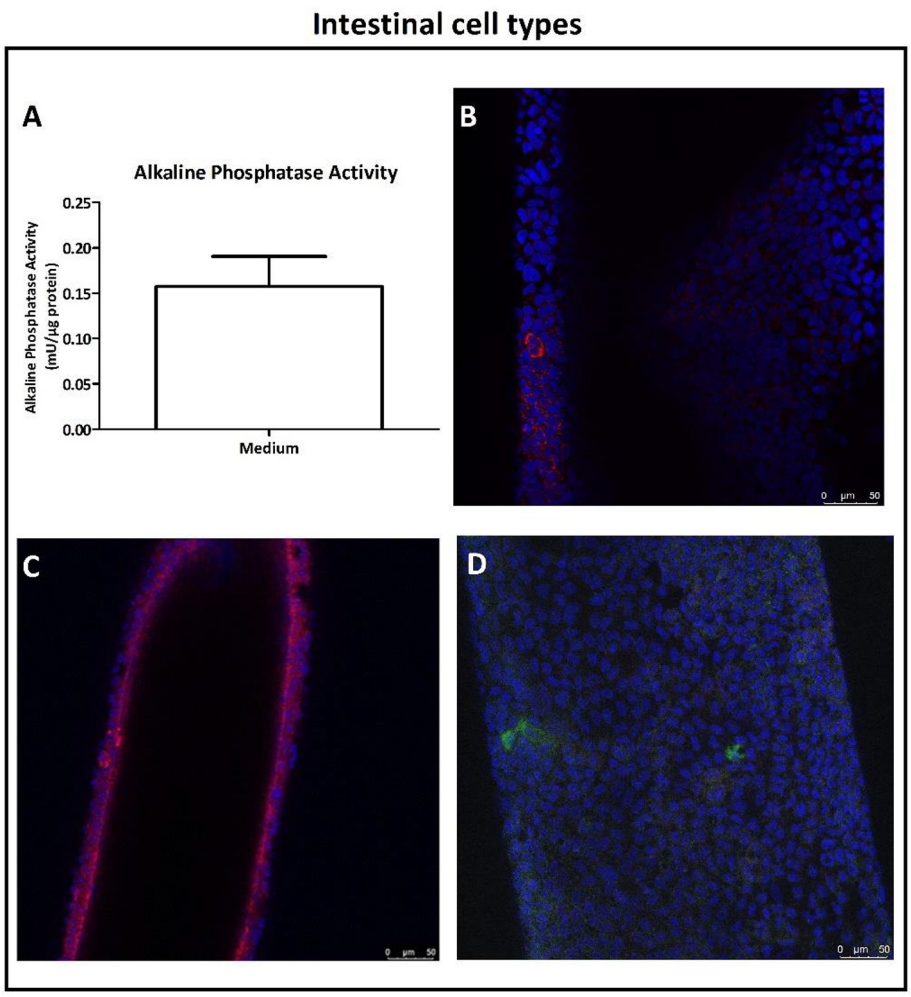

Fig. 6. Bioengineerd intestinal tubules differentiate into enterocyte-like cells, enteroendocrine cells, Paneth cells and stem cells. (A) Alkaline phosphatase activity per µg protein was determined for Caco-2 seeded on HFM (mean: 0.1065 ALP activity/µg protein). Data is expressed in mean ± standard error of the mean of at least three independent experiments. B,C and D show a representative confocal microscopic image of coated Caco-2 seeded HFM with 7 days of shear stress. In blue the DAPI staining of nuclei, in red positive staining for Chromogranin A (B), in red positive staining for lysozyme (C) and in green positive staining for leucine-rich repeat-containing G-protein coupled receptor 5. (For interpretation of the references to colour in this figure legend, the reader is referred to the web version of this article.)

formation compared to control. Caco-2 cells cultured as bioengineered intestinal tubules differentiate in enterocyte-like cells as shown by the induction of ALP activity. In future experiments it could be worthwhile to compare ALP levels between TW and the bioengineered intestinal tubules with respect to Caco-2 cell differentiation. This comparison could be meaningful in cases of screening of products or components would be specifically screened for their impact on ALP-activity. However, it must be taken into account that ALP-activity of Caco-2 cells is dependent on culture conditions and assay protocols which differ substantially between TW and bioengineered intestinal tubules cultures (Briske-Anderson et al., 1997).

In vivo, the ECM is an important player in the epithelial cell shape, gene expression, adhesion, migration, proliferation and apoptosis (Li and Thompson, 2003; Schophuizen et al., 2015; Hidalgo et al., 1989). The ECM is a mixture of different types of collagen, laminins, entactin and heparan sulfate proteoglycans (Schreider et al., 2002; Bosman and Stamenkovic, 2003). Collagen type IV is the main component in the basement membrane and is important for structural support along with key signaling for various physiological functions (Karsdal, 2016). ECM-coated HFM showed to support cells to form a tighter barrier and to differentiate better compared to uncoated HFM. It was previously demonstrated that collagen IV allowed Caco-2 cells to have increased activity of brush border enzymes and cell spreading, integrin dependency was postulated (Basson et al., 1996a). As such, integrin α5β1 has shown to increase the activity of PI3K/Akt signaling pathway (Lee and Juliano, 2000). Downstream, PI3K/Akt signaling upregulates mTOR and, in turn, mTOR is shown to support the Paneth and goblet cells population (Bailis and Pear, 2012; Zhou et al., 2016). Therefore, we postulate that in our model the ECM-integrin interaction may play a key role leading to the improved Caco-2 cell monolayer differentiation.

Caco-2 cells are known to spontaneously differentiate post-confluency in 2–3 weeks (Ferruzza et al., 2012; Pinto et al., 1983). Previously, it has been shown that variable seeding densities affect the expression levels of essential proteins, including human peptide transporter-1 and P-glycoprotein efflux pump. Higher seeding densities even led to multilayer formations (Sambuy et al., 2005; Behrens and Kissel, 2003). During model development, it is important to determine the optimal seeding density, as many factors, such as supplier, passage number and passaging, can influence the level of differentiation and polarization (Sambuy et al., 2005). Here, we show that $1.0*10^6$ cells/HFM was most optimal in prominent epithelial barrier formation.

As a final parameter, we studied the effect of shear stress, for which addition of a physiological flow (0.006 dyne/cm^2) was most optimal when exposure time was set to be the final 7 days, enlarging the surface for possible compound uptake, bringing the morphology closer to the human *in vivo* structure. Mechanical forces are known to induce cellular responses affecting *e.g.* proliferation and differentiation (Gayer and Basson, 2009). Basson et al. showed that addition of shear stress resulted promotion of proliferation and modulation of differentiation in Caco-2 cells (Basson et al., 1996b). Under shear stress conditions, protein kinase C (PKC) and mitogen-activated protein kinase (MAPK) ERK are activated (Basson and Hong, 1995; Li et al., 2001; Chen et al., 1994). PKC promotes Paneth cell differentiation and MAPK-ERK promotes goblet cell over Paneth and stem cell differentiation *via* post-translationally suppression of the Wnt/β-catenin pathway (Nakanishi et al., 2016; Osaki and Gama, 2013). As the Caco-2 cells originate from

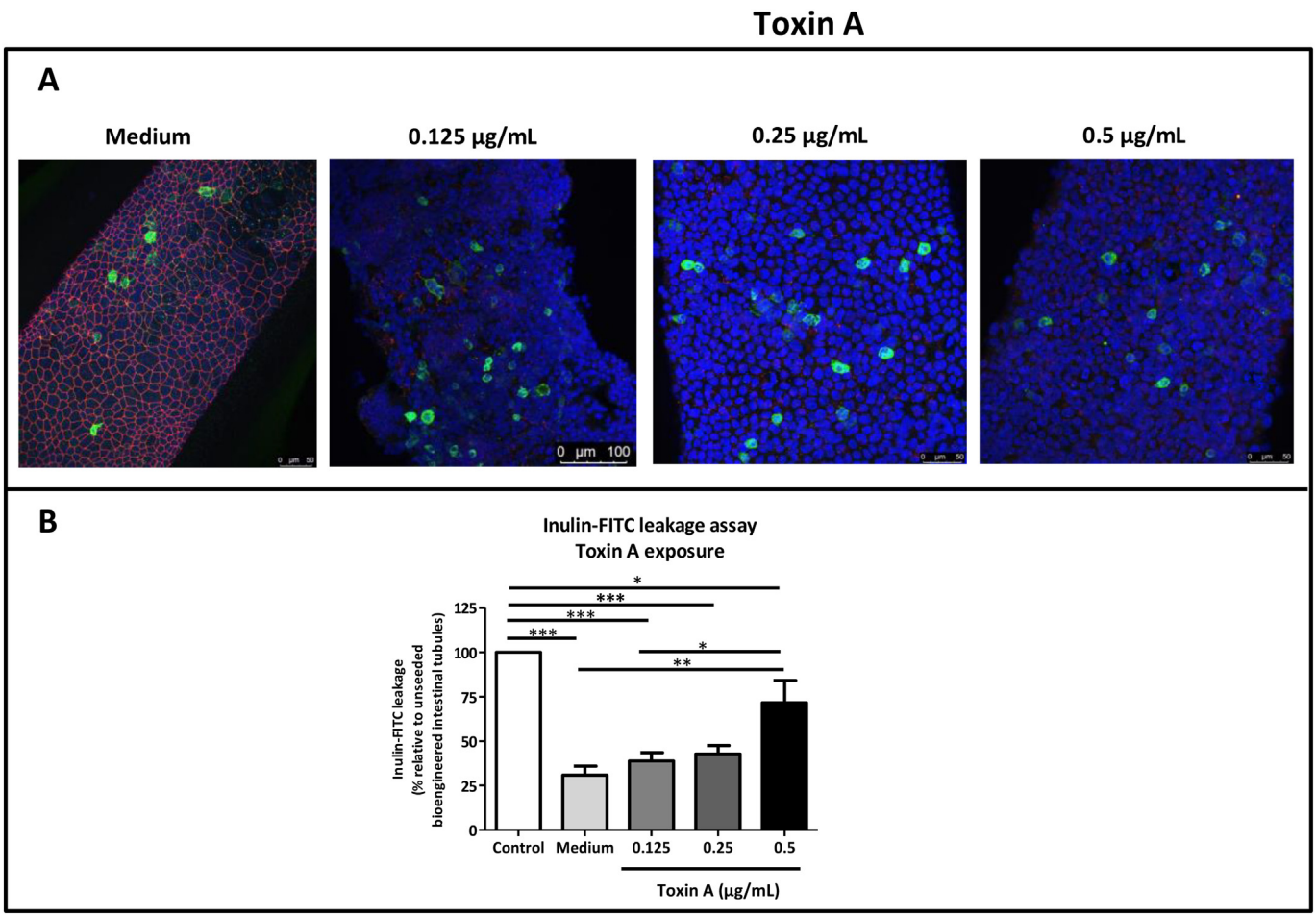

Fig. 7. Bioengineered intestinal tubules exposed to toxin A lose barrier function and show increased goblet cell presence. (A) representative confocal microscopic image of ECM-coated Caco-2 seeded hollow fiber membrane with 7 days of shear stress exposed to 24 h of Toxin A (left medium, middle left 0.125 µg/mL, middle right 0.25 µg/mL and right 0.5 µg/mL) In blue the DAPI staining of nuclei, immunostaining in green for mucin-2 and in red for zonula occludens-1. (B) Inulin-FITC paracellular leakage, data are presented relative to control as mean ± SEM of 7 independent experiments and was tested for significance to unseeded control HFM. $^{*}P < .05$, $^{**}P < 0.005$, $^{***}P < 0.001$ using one-way ANOVA. (For interpretation of the references to colour in this figure legend, the reader is referred to the web version of this article.)

colon carcinoma and colorectal cancer is associated with an activating mutation in the Wnt cascade (Reya and Clevers, 2005), we hypothesize that addition of shear stress suppresses the Wnt-cascade in our model thereby counteracting the Wnt-cascade activation originally present in the carcinoma cell line. This is supported by our cell differentiation as in our model we show goblet cell expression.

The crosstalk between the pathways postulated, result in the differentiation of the four main cell types: enterocyte, goblet, Paneth, enteroendocrine cells. Remarkably, even stem cells were observed as could be concluded from the $LGR5^{+}$ positivity. Each cell type plays its own role *in vivo* as such, enterocytes are specialized in transporting *e.g.* nutrients by expressing specific transporters on the luminal side. Defects may cause insufficient uptake of nutrition (Turner, 2015). Goblet cells produce mucus to form a barrier over the intestinal epithelium preventing direct contact and adhesion of pathogens (Turner, 2015). Paneth cells secrete antimicrobial peptides *e.g.* lysozyme and defensins (Turner, 2015). Enteroendocrine cells secrete a variety of hormones and signal molecules and thereby play a key role in regulating the digestive process (Sternini et al., 2008). Finally, stem cells are undifferentiated cells that can differentiate in mature epithelial cell types, important for the self-renewal of the epithelial cells (Umar, 2010). The presence of multiple cell types upon differentiation of Caco-2 cells on our bioengineered intestinal tubules is a promising improvement towards physiological relevance of our model that warrants translational studies in the future. Before, co-cultivation with the HT-29 cell line and its clones was recommended to introduce goblet cells in Caco-2 models (Wikman-Larhed and Artursson, 1995). Here, it is shown that a mono-culture of Caco-2 cells enables the possibility to study effects on goblet cells. To further evaluate the physiological resemblance, translational data and human tissue will be required for a direct comparison. One of the great advantages of organoid cultures is the differentiation into all intestinal cell types, just as we observed for the Caco-2 cells in this model (Zachos et al., 2016). Compared to organoid cultures, Caco-2 cultures are easy to culture, cost efficient, and accessible at both the apical and basolateral membrane for exposure studies. However, the colon carcinoma-origin of Caco-2 cells remains a limitation to their physiological relevance, because molecular pathways including Wnt/β-catenin and PI3K/AKT signaling can be altered. These pathways are involved in important cellular processes, such as cell proliferation and differentiation, control of metabolism and apoptosis that can be disrupted in colonic cancer (De Rosa et al., 2015). Therefore, cultivating intestinal organoids on the ECM-coated HFM-format might be a promising future direction for our model to allow for studying intestinal development.

After setting the microenvironment, After setting the microenvironment, it was translated to the TW inserts and a direct comparison for the barrier formation was done to further establish our model for studying intestinal permeability, as Caco-2 cells cultured on TW

inserts are considered the gold standard for *in vitro* intestinal permeability studies (Tan et al., 2018). No significant difference was detected in barrier formation between the bioengineered intestinal tubules and TW. Therefore, we believe that the bioengineered tubule is a suitable *in vitro* model to study intestinal permeability. Thereafter, the applicability of the bioengineered intestinal tubules in toxicity screenings was demonstrated for Tox A, a toxin produced by *Clostridium difficile* residing in the human small intestine. *Clostridium difficile* infection is the leading cause of healthcare associated diarrhea (Kuehne et al., 2010). Previously, Tox A showed to impair the Caco-2 monolayer integrity upon 4-fold higher ($2\,\mu g/mL^{-1}$) concentration (Zimmermann et al., 2018). We observed a complete disruption of the ZO-1 network for all Tox A concentrations and the highest concentration (0.5 μg/mL) leading to a significant increase in inulin-FITC leakage compared to medium and the lowest concentration Tox A exposed bioengineered intestinal tubules. These results are in line with previous finding supporting the barrier disruptive effect of Tox A. It has been shown in HT29-C1.16E cells that Tox A inhibits exocytosis of MUC2, this might explain the slight increase in positive MUC2 staining as MUC2 is no longer excreted (Branka et al., 1997). In this paper applicability of the model was shown for toxins by Tox A exposure. The highest concentration of Tox A resulted in a window able to detect beneficial and detrimental effects upon additional exposures of *e.g.* novel proteins. Next to evaluation of the functional barrier, assessment of the innate inflammatory and first-line defence response in the near future is of interest. Previous work already indicated that co-cultures between Caco-2 cells and immune cells show bi-directional interactions impacting on barrier, first-line defence and immune responses (Gavrovic-Jankulovic and Willemsen, 2015). In future work, bioengineered intestinal tubule cultures should apply the learnings from the TW co-culture models to increase the functional relevance of the model. The bioengineered intestinal tubules will have great applicability opportunities also beyond toxin screenings, *e.g.* in studying allergen penetration, drug absorption and novel food discovery.

In conclusion, addition of physiological parameters such as ECM-coating and flow, improved the phenotype and morphology of Caco-2 cells resulting in differentiated intestinal tubules. The presence of enterocyte, goblet, Paneth, enteroendocrine and stem cells was shown along with villi-like structures. These properties are not all present in conventional Caco-2 cultures, resulting in a model closer to the human physiology. Furthermore, applicability of the novel model after toxin exposure was shown, but this goes beyond toxins and will find its use as drug and nutrient screening tool.

Supplementary data to this article can be found online at https://doi.org/10.1016/j.tiv.2019.04.019.

Author contributions

PGMJ, AvG, SE and LWV conducted experimental work. PGMJ, JvB, RM and PJ designed experiments. PGMJ wrote and revised manuscript. JvB, JG, RM, HW reviewed and revised the manuscript.

Conflict of interest

Authors have no relevant conflict of interest to declare. This work was supported by the Dutch Ministry of Economic Affairs program TKI-AF under grant 15,269: Sustainable Future Proteins-Focus on nutritional and health promoting quality. The views expressed in this manuscript are those of the authors and do not necessarily reflect the position or policy of funding organizations: Cargill, La Saffre, PepsiCo, BASF, Mimetas, Proti-Farm, Danone Nutricia Research, Quorn Foods, Darling Ingredients, Roquette and AVEBE.

Acknowledgements

This work was supported by the Dutch Ministry of Economic Affairs program TKI-AF under grant 15269: Sustainable Future Proteins-Focus on nutritional and health promoting quality. The views expressed in this manuscript are those of the authors and do not necessarily reflect the position or policy of funding organizations: Cargill, La Saffre, PepsiCo, BASF, Mimetas, Proti-Farm, Danone Nutricia Research, Quorn Foods, Darling Ingredients, Roquette and AVEBE. Authors thank Silvia Fattorini for her contribution.

References

Alias, M.A., Buenzli, P.R., 2017. Modeling the effect of curvature on the collective behavior of cells growing new tissue. Biophys. J. 112 (1), 193–204.
Azadbakht, M., Madaeni, S.S., Sahebjamee, F., 2011. Biocompatibility of polyethersulfone membranes for cell culture systems. Eng. Life Sci. 11 (6), 629–635.
Bailis, W., Pear, W.S., 2012. Notch and PI3K: how is the road traveled? Blood 120 (7), 1349–1350.
Bardal, S., Waechter, J., Martin, D., 2010. Applied Pharmacology E-Book. Elsevier Health Sciences.
Basson, M.D., Hong, F., 1995. Modulation of human Caco-2 intestinal epithelial cell phenotype by protein kinase C inhibitors. Cell Biol. Int. 19 (12), 1025–1032.
Basson, M.D., Turowski, G., Emenaker, N.J., 1996a. Regulation of human (Caco-2) intestinal epithelial cell differentiation by extracellular matrix proteins. Exp. Cell Res. 225 (2), 301–305.
Basson, M.D., Di Li, G., Hong, F., Han, O., Sumpio, B.E., 1996b. Amplitude-dependent modulation of brush border enzymes and proliferation by cyclic strain in human intestinal Caco-2 monolayers. J. Cell. Physiol. 168 (2), 476–488.
Behrens, I., Kissel, T., 2003. Do cell culture conditions influence the carrier-mediated transport of peptides in Caco-2 cell monolayers? Eur. J. Pharm. Sci. 19 (5), 433–442.
Bosman, F.T., Stamenkovic, I., 2003. Functional structure and composition of the extracellular matrix. J. Pathol. 200 (4), 423–428.
Boussios, S., Pentheroudakis, G., Katsanos, K., Pavlidis, N., 2012. Systemic treatment-induced gastrointestinal toxicity: incidence, clinical presentation and management. Ann. Gastroenterol. 25 (2), 106.
Branka, J.E., Vallette, G., Jarry, A., Bou-Hanna, C., Lemarre, P., Van, P.N., et al., 1997. Early functional effects of Clostridium difficile toxin A on human colonocytes. Gastroenterology 112 (6), 1887–1894.
Briske-Anderson, M.J., Finley, J.W., Newman, S.M., 1997. The influence of culture time and passage number on the morphological and physiological development of Caco-2 cells. Proc. Soc. Exp. Biol. Med. 214 (3), 248–257.
Chen, Q., Kinch, M.S., Lin, T.H., Burridge, K., Juliano, R., 1994. Integrin-mediated cell adhesion activates mitogen-activated protein kinases. J. Biol. Chem. 269 (43), 26602–26605.
Chen, C., Jochems, P., Salz, L., Schneeberger, K., Penning, L.C., van de Graaf, S.F., et al., 2018. Bioengineered bile ducts recapitulate key cholangiocyte functions. Biofabrication 10 (3) 034103.
Clause, K.C., Liu, L.J., Tobita, K., 2010. Directed stem cell differentiation: the role of physical forces. Cell Commun. Adhes. 17 (2), 48–54.
De Rosa, M., Pace, U., Rega, D., Costabile, V., Duraturo, F., Izzo, P., et al., 2015. Genetics, diagnosis and management of colorectal cancer. Oncol. Rep. 34 (3), 1087–1096.
Deng, X., Zhang, G., Shen, C., Yin, J., Meng, Q., 2013. Hollow fiber culture accelerates differentiation of Caco-2 cells. Appl. Microbiol. Biotechnol. 97 (15), 6943–6955.
DePestel, D.D., Aronoff, D.M., 2013. Epidemiology of Clostridium difficile infection. J. Pharm. Pract. 26 (5), 464–475.
Ferruzza, S., Rossi, C., Scarino, M.L., Sambuy, Y., 2012. A protocol for differentiation of human intestinal Caco-2 cells in asymmetric serum-containing medium. Toxicol. in Vitro 26 (8), 1252–1255.
Funk, C., Roth, A., 2017. Current limitations and future opportunities for prediction of DILI from in vitro. Arch. Toxicol. 91 (1), 131–142.
Gavrovic-Jankulovic, M., Willemsen, L.E., 2015. Epithelial models to study food allergen-induced barrier disruption and immune activation. Drug Discov. Today Dis. Model. 17, 29–36.
Gayer, C.P., Basson, M.D., 2009. The effects of mechanical forces on intestinal physiology and pathology. Cell. Signal. 21 (8), 1237–1244.
Hidalgo, I.J., Raub, T.J., Borchardt, R.T., 1989. Characterization of the human colon carcinoma cell line (Caco-2) as a model system for intestinal epithelial permeability. Gastroenterology 96 (3), 736–749.
Hilgendorf, C., Spahn-Langguth, H., Regårdh, C.G., Lipka, E., Amidon, G.L., Langguth, P., 2000. Caco-2 versus Caco-2/HT29-MTX co-cultured cell lines: Permeabilities via diffusion, inside-and outside-directed carrier-mediated transport. J. Pharm. Sci. 89 (1), 63–75.
Holley, T., Bowe, G., Campia, I., Belz, S., Berggren, E., Janusch-Roi, A., et al., 2016. Accelerating progress in the replacement, reduction and refinement of animal testing through better knowledge sharing. EUR. https://doi.org/10.2788/243531. (print).
Honek, J., 2017. Preclinical research in drug development. Medical Writing 26, 5–8.
Huh, D., Torisawa, Y.-S., Hamilton, G.A., Kim, H.J., Ingber, D.E., 2012. Microengineered physiological biomimicry: organs-on-chips. Lab Chip 12 (12), 2156–2164.
Jain, A.K., Singh, D., Dubey, K., Maurya, R., Mittal, S., Pandey, A.K., 2017. Models and methods for In vitro toxicity. In: Vitro Toxicology, pp. 45.
Karsdal, M., 2016. Biochemistry of Collagens, Laminins and Elastin: Structure, Function and Biomarkers. Academic Press.
Kim, H.J., Ingber, D.E., 2013. Gut-on-a-Chip microenvironment induces human intestinal cells to undergo villus differentiation. Integr. Biol. 5 (9), 1130–1140.
Kim, H.J., Huh, D., Hamilton, G., Ingber, D.E., 2012. Human gut-on-a-chip inhabited by

microbial flora that experiences intestinal peristalsis-like motions and flow. Lab Chip 12 (12), 2165–2174.
Kuehne, S.A., Cartman, S.T., Heap, J.T., Kelly, M.L., Cockayne, A., Minton, N.P., 2010. The role of toxin a and toxin B in Clostridium difficile infection. Nature 467 (7316), 711.
Le Ferrec, E., Chesne, C., Artusson, P., Brayden, D., Fabre, G., Gires, P., et al., 2001. In vitro models of the intestinal barrier. Atla 29, 649–668.
Lea, T., 2015. Caco-2 Cell Line. The Impact of Food Bioactives on Health. Springer, pp. 103–111.
Lee, J.W., Juliano, R., 2000. α5β1 integrin protects intestinal epithelial cells from apoptosis through a phosphatidylinositol 3-kinase and protein kinase B–dependent pathway. Mol. Biol. Cell 11 (6), 1973–1987.
Lentle, R., Janssen, P., 2008. Physical characteristics of digesta and their influence on flow and mixing in the mammalian intestine: a review. J. Comp. Physiol. B. 178 (6), 673–690.
Li, A., Thompson, R., 2003. Basement Membrane Components. BMJ Publishing Group.
Li, W., Duzgun, A., Sumpio, B.E., Basson, M.D., 2001. Integrin and FAK-mediated MAPK activation is required for cyclic strain mitogenic effects in Caco-2 cells. Am. J. Physiol. Gastrointest. Liver Physiol. 280 (1), G75–G87.
McKee, C., Chaudhry, G.R., 2017. Advances and challenges in stem cell culture. Colloids Surf. B: Biointerfaces 159, 62–77.
Meunier, V., Bourrie, M., Berger, Y., Fabre, G., 1995. The human intestinal epithelial cell line Caco-2; pharmacological and pharmacokinetic applications. Cell Biol. Toxicol. 11 (3–4), 187–194.
Murphy, C.M., O'Brien, F.J., 2010. Understanding the effect of mean pore size on cell activity in collagen-glycosaminoglycan scaffolds. Cell Adhes. Migr. 4 (3), 377–381.
Murphy, C.M., Haugh, M.G., O'Brien, F.J., 2010. The effect of mean pore size on cell attachment, proliferation and migration in collagen–glycosaminoglycan scaffolds for bone tissue engineering. Biomaterials 31 (3), 461–466.
Nakanishi, Y., Reina-Campos, M., Nakanishi, N., Llado, V., Elmen, L., Peterson, S., et al., 2016. Control of paneth cell fate, intestinal inflammation, and tumorigenesis by PKCλ/ι. Cell Rep. 16 (12), 3297–3310.
Ni, M., Teo, J.C., bin Ibrahim, M.S., Zhang, K., Tasnim, F., Chow, P.-Y., et al., 2011. Characterization of membrane materials and membrane coatings for bioreactor units of bioartificial kidneys. Biomaterials 32 (6), 1465–1476.
Osaki, L., Gama, P., 2013. MAPKs and signal transduction in the control of gastrointestinal epithelial cell proliferation and differentiation. Int. J. Mol. Sci. 14 (5), 10143–10161.
Philpott, H., Nandurkar, S., Lubel, J., Gibson, P., 2014. Republished: drug-induced gastrointestinal disorders. Postgrad. Med. J. 90 (1065), 411–419.
Pinto, M.R.-L.S., Appay, M.D., Kedinger, M., Triadou, N., Dussaulx, E., Lacroix, B., Simon-Assmann, P., Haffen, K., Fogh, J., Zweibaum, A., 1983. Enterocyte-like differentiation and polarization of the human colon carcinoma cell line Caco-2 in culture. Biol. Cell. 47, 7.
Press, B., Di Grandi, D., 2008. Permeability for intestinal absorption: Caco-2 assay and related issues. Curr. Drug Metab. 9 (9), 893–900.
Pusztaszeri, M.P., Genta, R.M., Cryer, B.L., 2007. Drug-induced injury in the gastrointestinal tract: clinical and pathologic considerations. Nat. Rev. Gastroenterol. Hepatol. 4 (8), 442.
Reya, T., Clevers, H., 2005. Wnt signalling in stem cells and cancer. Nature 434 (7035), 843.
Sambuy, Y., De Angelis, I., Ranaldi, G., Scarino, M., Stammati, A., Zucco, F., 2005. The Caco-2 cell line as a model of the intestinal barrier: influence of cell and culture-related factors on Caco-2 cell functional characteristics. Cell Biol. Toxicol. 21 (1), 1–26.
Schophuizen, C.M., De Napoli, I.E., Jansen, J., Teixeira, S., Wilmer, M.J., Hoenderop, J.G., et al., 2015. Development of a living membrane comprising a functional human renal proximal tubule cell monolayer on polyethersulfone polymeric membrane. Acta Biomater. 14, 22–32.
Schreider, C., Peignon, G., Thenet, S., Chambaz, J., Pinçon-Raymond, M., 2002. Integrin-mediated functional polarization of Caco-2 cells through E-cadherin—actin complexes. J. Cell Sci. 115 (3), 543–552.
Sternini, C., Anselmi, L., Rozengurt, E., 2008. Enteroendocrine cells: a site of 'taste'in gastrointestinal chemosensing. Curr. Opin. Endocrinol. Diabetes Obesity 15 (1), 73.
Stewart, A.S., Pratt-Phillips, S., Gonzalez, L.M., 2017. Alterations in intestinal permeability: the role of the "Leaky Gut" in health and disease. J. Equine Veterin. Sci. 52, 10–22.
Sun, H., Chow, E.C., Liu, S., Du, Y., Pang, K.S., 2008. The Caco-2 cell monolayer: usefulness and limitations. Expert Opin. Drug Metab. Toxicol. 4 (4), 395–411.
Tan, H.-Y., Trier, S., Rahbek, U.L., Dufva, M., Kutter, J.P., Andresen, T.L., 2018. A multi-chamber microfluidic intestinal barrier model using Caco-2 cells for drug transport studies. PLoS One 13 (5), e0197101.
Trietsch, S.J., Naumovska, E., Kurek, D., Setyawati, M.C., Vormann, M.K., Wilschut, K.J., et al., 2017. Membrane-free culture and real-time barrier integrity assessment of perfused intestinal epithelium tubes. Nat. Commun. 8 (1), 262.
Turner, J.R., 2015. Epithelia and gastrointestinal function. In: Yamada's Textbook of Gastroenterology, pp. 317–329.
Umar, S., 2010. Intestinal stem cells. Curr. Gastroenterol. Rep. 12 (5), 340–348.
Webster, M., Witkin, K.L., Cohen-Fix, O., 2009. Sizing up the nucleus: nuclear shape, size and nuclear-envelope assembly. J. Cell Sci. 122 (10), 1477–1486.
Werner, M., Blanquer, S.B., Haimi, S.P., Korus, G., Dunlop, J.W., Duda, G.N., et al., 2017. Surface curvature differentially regulates stem cell migration and differentiation via altered attachment morphology and nuclear deformation. Adv. Sci. 4 (2), 1600347.
Wikman-Larhed, A., Artursson, P., 1995. Co-cultures of human intestinal goblet (HT29-H) and absorptive (Caco-2) cells for studies of drug and peptide absorption. Eur. J. Pharm. Sci. 3 (3), 171–183.
Yue, B., 2014. Biology of the extracellular matrix: an overview. J. Glaucoma S20.
Zachos, N.C., Kovbasnjuk, O., Foulke-Abel, J., In, J., Blutt, S.E., De Jonge, H.R., et al., 2016. Human enteroids/colonoids and intestinal organoids functionally recapitulate normal intestinal physiology and pathophysiology. J. Biol. Chem. 291 (8), 3759–3766.
Zhou, Y., Rychahou, P., Wang, Q., Weiss, H.L., Evers, B.M., 2016. TSC2/mTORC1 signaling controls Paneth and goblet cell differentiation in the intestinal epithelium. Cell Death Dis. 6 (2), e1631.
Zimmermann, C., Eaton, A., Lanter, B., Roper, J., Hurley, B., Delaney, B., 2018. Extended exposure duration of cultured intestinal epithelial cell monolayers in characterizing hazardous and non-hazardous proteins. Food Chem. Toxicol. 115 (5), 451–459.